



# Bachelor Thesis

---

Measurement concepts for determining nitrogen oxides  
at a molten salt plant

Department 3: Chemistry and Biotechnology  
Fachhochschule Aachen  
Campus Jülich

Submitted by

**TAHA QADA**

Erstbetreuer

**PROF. DR. YI ZHANG**

Zweitbetreuerin

**DR.-ING. BÄRBEL SCHLÖGL-KNOTHE**  
**M.SC.SOPHIE KAPPERTZ**

Jülich, 7. October 2025

## Declaration

I hereby declare that I have independently created and written the present work. Any citations, images, or diagrams that are not my own are appropriately referenced with sources.

No other sources or aids have been used.

---

Taha Qada



## Appreciations:

I would like to express my heartfelt gratitude to my first supervisor, Prof. Dr. Yi Zhang, for her guidance, trust, and insightful advice throughout the preparation of this Bachelor thesis. Her academic expertise and constant support have been of great value to me.

My sincere appreciation also goes to my second supervisor, Dr.-Ing. Bärbel Schlögl-Knothe, whose constructive feedback, and dedication have greatly contributed to the development and improvement of my work.

I am equally thankful to M.Sc. Sophie Kappertz for her kind assistance at DLR and for helping me to coordinate the organizational aspects of this project.

Lastly, I would like to thank the colleagues at DLR and at FH Aachen for their helpful input, collaboration, and support, which have accompanied me during the completion of this thesis.



## Table of Contents

<b>1. Introduction and Objective .....</b>	<b>1</b>
<b>2. Theory .....</b>	<b>2</b>
2.1 The molten salt loop.....	2
2.2 The role of molten salts (NaNO <sub>3</sub> /KNO <sub>3</sub> ) as ways to transfer and store heat. ...	4
2.3 Thermal decomposition of NaNO <sub>3</sub> /KNO <sub>3</sub> and formation of reactive gases .....	5
2.4 Risks Associated with NO <sub>x</sub> Presence and Safety Measures at the SALSA Facility	7
<b>3. Experimental part .....</b>	<b>8</b>
3.1 Current Installed NO <sub>x</sub> -Sensor.....	8
3.2 Analysis of Collected Measurement Data and Anomalies.....	13
Interpretation: 30.07.2024 .....	13
Interpretation: 19.08.2024.....	15
Interpretation: 19.09.2024 .....	16
Summary of NO <sub>x</sub> Sensor Behavior:.....	17
<b>4. Factors affecting sensor accuracy and alternative measurement concepts .....</b>	<b>18</b>
4.1 Potential Factor Affecting Sensor Accuracy .....	18
4.2 Adapted Techniques for NO <sub>x</sub> Detection under CST Operating Conditions .....	19
Working Principle of NDIR Method .....	19
Working Principle of the Chemiluminescence Method .....	20
Working Principle of NDUV Method.....	22
Working principle of electrochemical Method.....	23
4.3 Proposed Measurement Concept: .....	26
<b>5. Conclusion: .....</b>	<b>27</b>
<b>6. Reference .....</b>	<b>29</b>
<b>7. Appendix.....</b>	<b>32</b>
Appendix 1.....	32
Appendix 2.....	32
Appendix 3.....	33
Appendix 4.....	34
Appendix 5.....	36
Appendix6:.....	37



## Abbreviations and Symbols

CSP: Concentrated Solar Power

SALSA: Salzschnmelze Anlage

CST: Concentrated Solar Tower

HPMS-II: High Performance Molten Salt

EEA: European Environment Agency

TA-Luft: Technische Anleitung zur Reinhaltung der Luft

ASIC: Application-Specific Integrated Circuit

ECU: Electronic Control Unit

CAN: Controller Area Network

NDIR: Non-Dispersive Infrared

IR: Infrared

KNESTEL: Knestel Technologie & Elektronik GmbH

CLD: Chemiluminescence Detector

nCLD: nitric Chemiluminescence Detector

UV: Ultraviolet

SICK: SICK AG

GM: Gas Module

SIPROCESS: Siemens SIPROCESS Gas Analyzer

## 1. Introduction and Objective

Concentrated Solar Power (CSP) systems, and in particular tower-based configurations, have the advantage of combining renewable power generation with large scale thermal energy storage. This makes them suitable for continuous electricity supply and for improving the flexibility of renewable integration into the grid [1]. To achieve this, molten nitrate salts are commonly used as heat transfer and storage media due to their high thermal stability and ability to operate at elevated temperatures [2]. The SALSA loop in Jülich, Germany, was designed as an experimental facility to investigate such high temperature operation. It enables the testing of advanced receiver technologies, under realistic tower conditions at salt outlet temperatures up to 600 °C [2]. The facility is located in the Multifocus Tower in Jülich and uses the local heliostat field for solar irradiation, which consists of a large array of computer-controlled mirrors that follow the sun and continuously redirect sunlight to different levels of the tower and the receiver.

The facility consists of inlet and outlet tanks, a salt pump, and a central tube receiver that can be preheated using solar radiation from heliostats. During operation, molten salt is circulated through the receiver, where it absorbs concentrated solar energy, enabling realistic testing of key challenges such as salt melting and circulation, thermal stability, receiver start-up behavior, and efficiency. At the high operating temperatures of solar tower plants, molten nitrate salts can partially decompose and release nitrogen oxides (NO<sub>x</sub>), which are harmful air pollutants contributing to smog formation and acid rain. Monitoring NO<sub>x</sub> is therefore essential to ensure compliance with environmental regulations and to maintain the role of solar tower technology as a sustainable energy source. Continuous measurement also provides operators with critical information on gas emissions during plant operation, thereby supporting both safety and efficiency. Overall, the SALSA infrastructure offers the necessary environment to assess not only the functionality and performance of receiver systems but also the importance of reliable NO<sub>x</sub> monitoring for the long-term viability of molten salt based solar power plants [3].

The purpose of this thesis is to take a closer look at how nitrogen oxides (NO<sub>x</sub>) are measured in molten salt solar tower systems and to find ways of making this

monitoring more reliable. To begin with, the performance of the electrochemical sensor currently installed at the SALSA facility will be examined, with a particular focus on how accurately and consistently it reports data under real operating conditions. Special attention will be given to the irregularities that have already been observed in the measurement results, such as negative or fluctuating values, in order to understand their possible causes. Finally, based on the findings, the work will explore alternative solutions and propose a more robust approach to NO<sub>x</sub> monitoring. This will include identifying a sensor technology that is better suited to the plant's requirements and integrating it with a gas sampling and cooling system, ensuring accurate and dependable measurements for future operation.

## 2. Theory

### 2.1 The molten salt loop

In order to evaluate the formation and monitoring of NO<sub>x</sub> emissions, it is first necessary to understand the thermal processes to which molten salt is subjected in a solar tower system. The binary mixture of sodium nitrate (NaNO<sub>3</sub>) and potassium nitrate (KNO<sub>3</sub>), commonly referred to as solar salt, must be carefully melted, preheated, circulated, and maintained at a high temperature within the plant. Each step of this process from initial melting and preheating to circulation through the receiver affects the operating conditions under which thermal decomposition and gas release can occur. For this reason, it is essential to take a closer look at how the SALSA molten salt cycle works before NO<sub>x</sub> emissions can be discussed in detail [\[4\]](#).

The SALSA loop was developed as infrastructure for testing and operating high-temperature molten salt receiver systems under realistic tower conditions. It comprises all necessary subsystems, such as a storage tank, a salt pump, inlet and outlet vessels, and a control system that enables both steady-state operation and transient processes such as preheating, partial load operation, or emergency shutdown. Instead of a steam generator, an air cooler is integrated to dissipate the absorbed heat energy. This configuration enables flexible testing of receiver

prototypes, such as the HPMS-II tube receiver, at temperatures of up to 600 °C in the Multi-focus tower in Jülich [4].

The overall structure of the SALSA molten salt loop is shown in Figure 1, which combines view of the plant with a schematic process flow diagram. This provides an overview of the main components, including the salt tanks, the receiver, the salt cooler, and the auxiliary heater, as well as the piping system for molten salt.

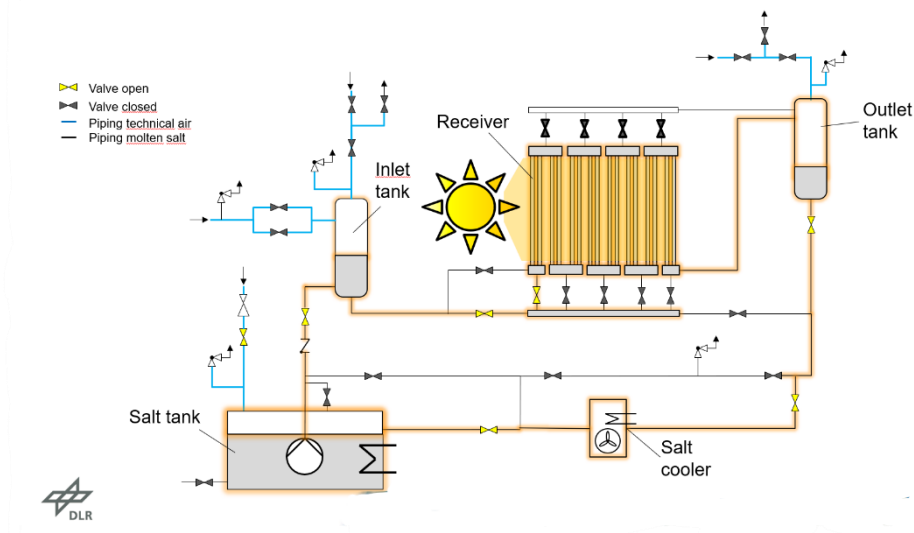


Figure 1: Overview of the SALSA molten salt loop. Schematic flow diagram showing the main components and process layout [4].

Once the receiver is prepared for solar operation, the filling process begins. The absorber pipes are preheated by heliostats to prevent condensation and thermal shocks. First, the molten salt is pumped from the bottom to fill the pipes and the inlet tank. After that, the flow can be directed through the bypass line. In the last step, by changing the valves, the salt is pumped into the receiver from bottom to top. Once the receiver is filled, the valves are switched so that the salt flows through the serpentine tubes of the receiver and then back through the outlet tank to the main salt tank. During this phase, the outlet tank is pressurized with synthetic air and the receiver is filled from the bottom up to prevent air pockets. This process ensures a stable salt flow and prevents local overheating of the pipes [4].

During daily operation, the receiver is heated by the solar radiation reflected by the heliostats. The molten salt absorbs the incident heat by flowing through the receiver and transports it through the circuit. At the end of operation, the receiver is carefully

depressurized and emptied to minimize thermal stress, and the salt is returned to the tank in a controlled manner. To ensure safety, the SALSA plant also defines various operating conditions and emergency procedures that can be activated if necessary [4].

## 2.2 The role of molten salts (NaNO<sub>3</sub>/KNO<sub>3</sub>) as ways to transfer and store heat.

In concentrated solar tower (CST) plants, one of the main engineering challenges is to capture solar radiation, transport the absorbed heat to the power block, and store it efficiently for later use. A binary eutectic mixture of sodium nitrate (NaNO<sub>3</sub>) and potassium nitrate (KNO<sub>3</sub>), commonly known as Solar Salt, has become the preferred medium for this purpose. The standard composition is approximately 60 % NaNO<sub>3</sub> and 40 % KNO<sub>3</sub> by weight, which provides an optimal balance of melting point, thermal stability, and cost [5]. The main thermophysical properties of Solar Salt are summarized in Table 1

Property	Value / Range	Notes / Relevance
<b>Composition</b>	60 % NaNO <sub>3</sub> , 40 % KNO <sub>3</sub> (by weight)	Binary eutectic mixture
<b>Melting point</b>	~220 °C	Ensures relatively easy liquefaction
<b>Maximum stability temperature</b>	~565 °C (under normal operation)	Above this, thermal decomposition accelerates
<b>Specific heat capacity</b>	~1.5 kJ/kg·K (at 300–565 °C)	Determines energy storage density
<b>Density (liquid phase)</b>	~1800–1900 kg/m <sup>3</sup>	High volumetric storage capacity
<b>Vapor pressure</b>	Very low (< 1 bar at operating temps)	Enables operation at near-atmospheric pressure
<b>Thermal conductivity</b>	~0.5 W/m·K	Moderate, sufficient for heat transfer
<b>Viscosity</b>	2–4 mPa·s (in liquid range)	Allows stable pumping in pipelines

Table 1: Key properties of Solar Salt (NaNO<sub>3</sub>/KNO<sub>3</sub>, 60/40 wt%) [5].

Solar Salt fulfils a dual function in CST systems: it acts both as a heat transfer fluid and as a thermal energy storage medium. Its melting point lies around 220 °C, low enough to be melted and circulated without excessive preheating, yet high enough to ensure stability under standard operation. Once liquefied, the mixture can be safely heated up to about 565 °C without significant decomposition, giving it a wide operational range suitable for solar tower receivers [5].

From a thermal perspective, Solar Salt offers a relatively high specific heat capacity (~1.5 kJ/kg·K at operating conditions) and density (~1800–1900 kg/m<sup>3</sup>), resulting in a large volumetric storage capacity [6][7]. This enables large-scale tanks to store several hours of thermal energy at grid-relevant scale. The salt also exhibits low vapor pressure, even at elevated temperatures, which allows operation at near-atmospheric pressure simplifying the design and reducing the cost of storage tanks, piping, and valves compared to pressurized fluids [8].

In addition to storage, the salt is continuously circulated through the receiver, absorbing concentrated solar radiation and transporting the heat through the system. Its viscosity remains moderate in the liquid state, enabling stable pumping over long piping networks. These combined properties of high heat capacity, low vapor pressure, and pumpable viscosity, make Solar Salt uniquely suitable for the combined tasks of transporting and storing energy in CST plants [9].

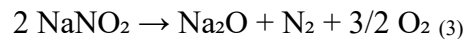
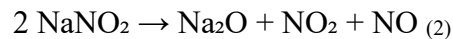
Finally, the mixture is economically viable because both sodium nitrate and potassium nitrate are widely produced for use in fertilizers, making them inexpensive and available. This industrial supply chain has facilitated the widespread adoption of Solar Salt in commercial-scale CSP plants. Current research is investigating modifications such as additives or alternative eutectic mixtures to further enhance stability and extend the temperature range [8], but the NaNO<sub>3</sub>/KNO<sub>3</sub> system remains the industry benchmark.

### 2.3 Thermal decomposition of NaNO<sub>3</sub>/KNO<sub>3</sub> and formation of reactive gases

The binary mixture of sodium nitrate (NaNO<sub>3</sub>) and potassium nitrate (KNO<sub>3</sub>), commonly known as Solar Salt, is thermally stable under normal operating conditions up to approximately 565 °C. Beyond this point, the nitrate ions become unstable and decomposition reactions begin to occur [10]. These initial reactions

generally take place between 500 and 600 °C, depending on heating rate and exposure time. The first step involves the partial reduction of nitrate ions ( $\text{NO}_3^-$ ) to nitrite ions ( $\text{NO}_2^-$ ), accompanied by the release of molecular oxygen ( $\text{O}_2$ ) (reaction 1) [11]. This oxygen release signals the onset of instability in the molten mixture.

When the operating temperature approaches or exceeds 600 °C, nitrites themselves become thermally unstable and undergo further decomposition, producing alkali oxides ( $\text{Na}_2\text{O}$ ,  $\text{K}_2\text{O}$ ), nitric oxide ( $\text{NO}$ ), and nitrogen dioxide ( $\text{NO}_2$ ) (reactions 2–3) [11-13]. Because  $\text{NO}$  is easily oxidized in oxygen-rich atmospheres,  $\text{NO}_2$  typically becomes the dominant nitrogen oxide species at advanced stages of decomposition. Experimental investigations confirm that above 500 °C, decomposition processes accelerate, resulting in measurable  $\text{NO}_x$  emissions and mass loss from the salt [12].



In addition to temperature, the chemical purity of the salt strongly influences its stability. Impurities present in commercially available solar salt can trigger premature decomposition. In particular, magnesium nitrate ( $\text{Mg}(\text{NO}_3)_2$ ), often found as a contaminant in fertilizer-quality salt, decomposes already between 290°C and 400°C, producing magnesium oxide, oxygen, and nitrogen oxides, and thus releasing  $\text{NO}_x$  before the main  $\text{NaNO}_3/\text{KNO}_3$  mixture reaches its own stability limit (reaction 4) [14].



In the SALSA loop, synthetic air, composed of nitrogen and oxygen, is used as a cover gas to establish the pressure required for circulating the molten solar salt through the piping and receiver system [4]. Nitrogen functions as an inert carrier gas, without any direct impact on decomposition or  $\text{NO}_x$  formation. Oxygen, in contrast, plays an active role in the chemical equilibrium of the system: while higher oxygen partial pressures can re-oxidize nitrites to nitrates, thereby stabilizing the melt, at temperatures above 600 °C nitrite ions nevertheless become unstable and decompose into corrosive oxide ions, releasing additional  $\text{NO}$  and  $\text{NO}_2$  [15-16].

Recent measurements also indicate that nitrite accumulation around 565 °C can shift the melting range and provide direct precursors for NO<sub>x</sub> generation under prolonged high-temperature exposure [17].

Altogether, oxygen release represents the first stage of nitrate breakdown, while NO and NO<sub>2</sub> appear as secondary products once nitrites decompose. Their concentrations increase with temperature, salt impurities, and the extent of degradation [12][11][17]. Understanding these effects is crucial for defining safe operating conditions in CST plants and for ensuring reliable NO<sub>x</sub> monitoring during operation.

## 2.4 Risks Associated with NO<sub>x</sub> Presence and Safety Measures at the SALSA Facility

The release of nitrogen oxides (NO and NO<sub>2</sub>) during salt decomposition is a serious concern because these gases affect both human health and the environment.

- Safety Risks

NO<sub>2</sub> is a very reactive gas. Even short-term exposure can irritate the eyes, throat, and lungs. People exposed for just a few hours may develop coughing, difficulty breathing, or worsening of asthma symptoms [18-19]. Children, elderly people, and people with lung diseases are the most sensitive. Clinical research shows that NO<sub>2</sub> can trigger asthma attacks, increase hospital admissions, and in some cases contribute to premature death. Long-term exposure, even at levels below 10 µg/m<sup>3</sup>, has been linked to the development of new cases of asthma in children and an increase in chronic lung disease in adults [18]. These effects mean that even relatively small concentrations of NO<sub>2</sub> inside or around a plant can create significant safety risks for workers and nearby communities.

- Environmental Risks

Nitrogen oxides also damage the environment once they are released into the air. NO and NO<sub>2</sub> take part in chemical reactions with sunlight and water vapor, leading to the formation of ground-level ozone and fine particles (smog) [19]. These

pollutants reduce air quality, harm vegetation, and affect crop yields. NO<sub>2</sub> also contributes to acid rain, which can damage forests, soils, and water systems.

At the European level, NO<sub>x</sub> emissions are closely monitored because of their large impact on both health and the environment. According to the European Environment Agency (EEA), nitrogen oxides are one of the key pollutants targeted under the National Emission Reduction Commitments Directive. However, several EU member states still struggle to meet their reduction targets, showing how difficult controlling NO<sub>x</sub> emissions can be [20]. This strict legal framework means that continuous NO<sub>x</sub> monitoring is not just good practice for plant safety but also necessary to comply with environmental regulations. For example, the German TA-Luft specifies emission limit values for NO<sub>x</sub> in industrial exhaust gases of 0.20 g/m<sup>3</sup>, or alternatively 0.35 g/m<sup>3</sup> with a maximum mass flow of 1.8 kg/h [21].

- Safety Measures

To ensure safe operation of the SALSA loop under high-temperature molten salt conditions, several precautionary measures are implemented. The system is equipped with a dedicated exhaust line that releases gases to the ambient atmosphere in a controlled manner, preventing overpressure inside the loop. During experimental campaigns, access to the test area is strictly prohibited in order to minimize exposure risks for personnel. In addition, a portable NO<sub>x</sub> analyzer is available, but it is not required during normal operation. It is only used for maintenance activities, for example when the salt tank is open and filled with molten salt, in order to provide real-time information on gas concentrations and ensure that operators are not exposed to hazardous levels of nitrogen oxides.

### 3. Experimental part

#### 3.1 Current Installed NO<sub>x</sub>-Sensor

To measure the emitted nitrogen oxides during molten salt operation, a dedicated NO<sub>x</sub>-Sensor was installed in the SALSA loop. The objective of this device is to provide continuous monitoring of the gas composition above the salt and to detect the presence of reactive species such as NO and NO<sub>2</sub>. The chosen sensor model was

originally designed for measuring  $\text{NO}_x$  in car's exhaust (Figure 2,3), but in Concentrated Solar Tower (CST) systems it operates under different conditions such as high temperatures and possible gas impurities. To understand its performance in this environment, it is important to first explain the basic measurement principle and the factors that influence it.

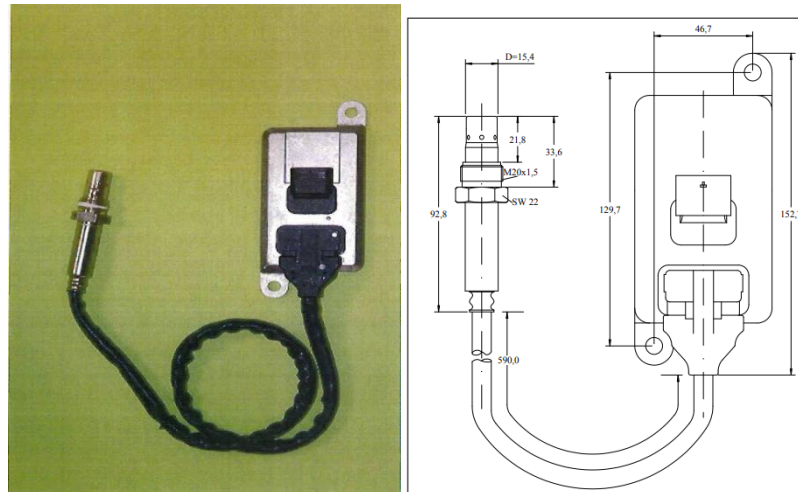


Figure 2: Installed electrochemical  $\text{NO}_x$  sensor (model 70501). Left: Photograph of the sensor with connector and cable. Right: Technical drawing with dimensions (in mm) [22].



Figure 3: Sensor element placed in the gas conduit.

- Operating Principle of the Installed NO<sub>x</sub>-Sensor

The NO<sub>x</sub> sensor used is based on an electrochemical design that combines multiple cavities with zirconia (ZrO<sub>2</sub>) pump cells and platinum electrodes (Figure 4). Its operation can be understood step by step by following the gas path inside the sensor.

After entering through the sampling inlet, the gas first passes through a diffusion barrier. This element regulates the gas flow and stabilizes the internal environment of the sensor. In the first cavity, the gas encounters a zirconia pump cell that removes excess oxygen by ionic transport, while a platinum electrode catalyses the oxidation of interfering species. This initial stage ensures that the sample gas is conditioned before measurement.

The treated gas then flows into the second cavity, where nitric oxide (NO) is catalytically reduced to nitrogen and oxygen. The oxygen produced during this reaction is extracted by a second zirconia pump. The resulting current is proportional to the transported oxygen, which directly reflects the concentration of NO in the sample. This principle is known as amperometric detection, as the measured current corresponds to the NO<sub>x</sub> level.

To improve sensitivity, an auxiliary zirconia pump further lowers the oxygen concentration in the second cavity to very low levels (below 10<sup>-3</sup> ppm). This minimizes background interference and enables accurate detection of trace NO<sub>x</sub>. The entire sensor body is maintained at approximately 750 °C by an integrated heater, since high temperature is required for zirconia to conduct oxygen ions. A thermocouple monitors this internal temperature to ensure stable operation.

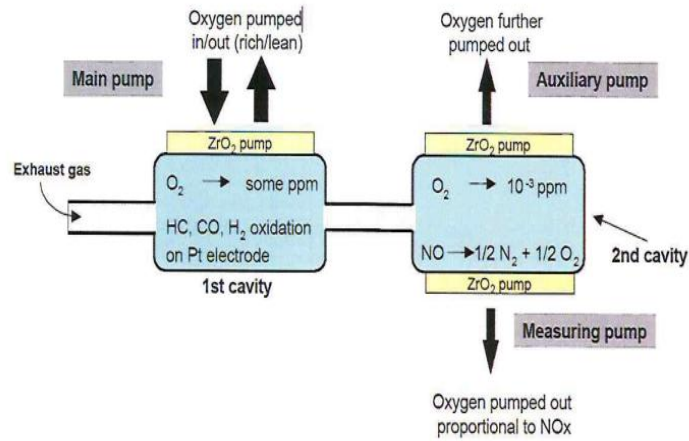


Figure 4: Schematic representation of the operating principle of the electrochemical NO<sub>x</sub> sensor [22].

On the electronic side, an ASIC chip processes the electrochemical signals and applies corrections for temperature effects and potential cross-sensitivities (Figure 5), the control signals and their functions are presented in [Appendix 1](#). The processed data are transmitted to the Electronic Control Unit (ECU) via a CAN bus interface (the main functions of the ECU are summarized in [Appendix 2](#)). The ECU supplies power, handles diagnostics, and ensures reliable communication with the overall system

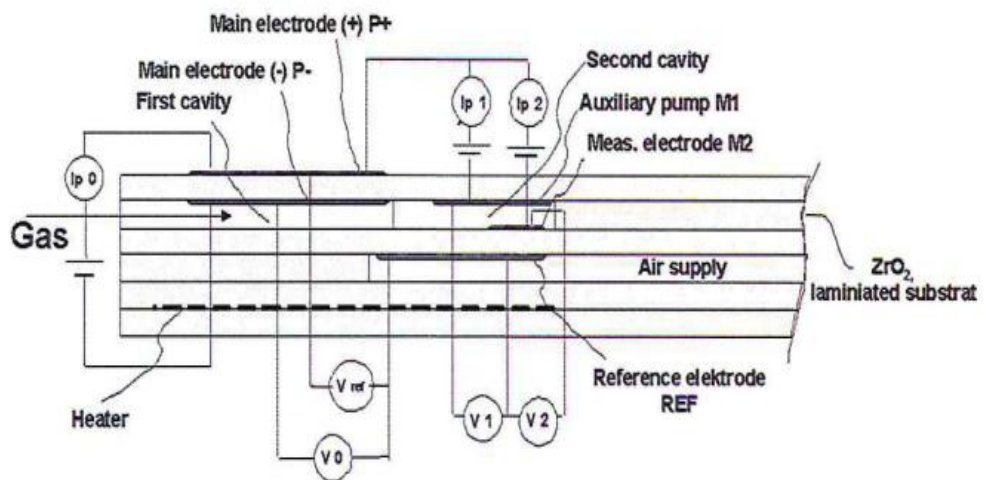


Figure 5: Control signals and internal structure of the electrochemical NO<sub>x</sub> sensor [22].

The measurement principle of this sensor therefore relies on the transport of oxygen ions through zirconia ceramics, with a stable reference electrode providing the necessary electrochemical potential. By combining ion pumping, catalytic reactions, and amperometric detection, the sensor delivers continuous and selective monitoring of NO<sub>x</sub> concentrations.

- Location of the sensor.

The sensor is installed inside the gas pipe and 180cm from the pipe's exhaust to the environment. A gas flow only passes through the exhaust pipe when the system needs to regulate its pressure. The inlet tank and outlet tank of the system are pressurized with synthetic air. A pressure regulator adjusts the pressure during operation and opens the corresponding valves to reduce it.

Its ECU is placed nearby but outside the hot zone to operate properly (Figure 6).

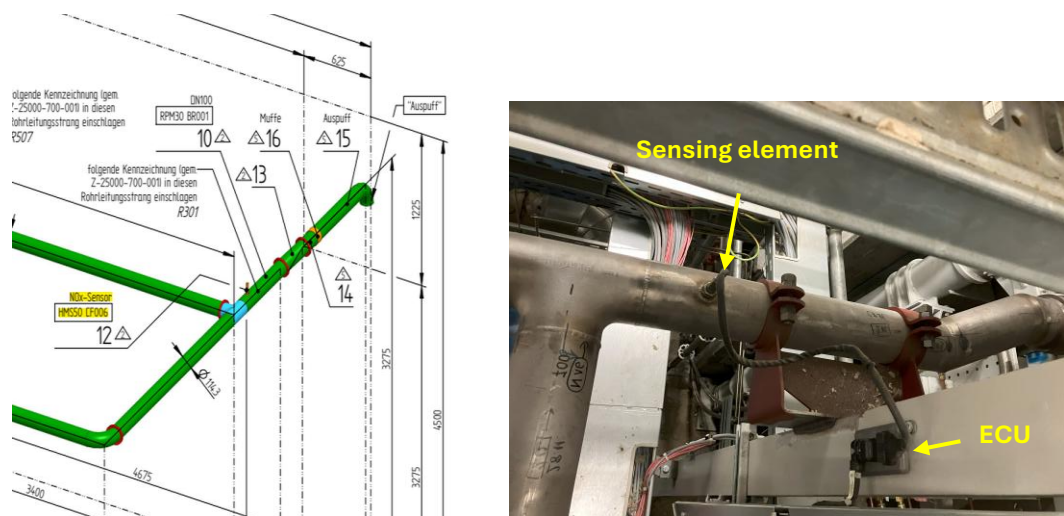


Figure 6: Integration of the NO<sub>x</sub>-Sensor (model 70501) in the gas conduit of the SALSA loop. Left: section of the piping diagram indicating the sensor location [23]. Right: photograph of the installation showing the sensing element inserted into the pipe and the electronic control unit (ECU) mounted nearby.

Understanding the measurement principle and the factors influencing sensor operation provides the foundation for evaluating its performance in the SALSA loop. Building on this, the next chapter presents the collected measurement data and examines the sensor's behavior under CST conditions, where commissioning and

initial test operation revealed irregularities such as negative concentration readings and fluctuating signals.

### 3.2 Analysis of Collected Measurement Data and Anomalies.

#### Interpretation: 30.07.2024

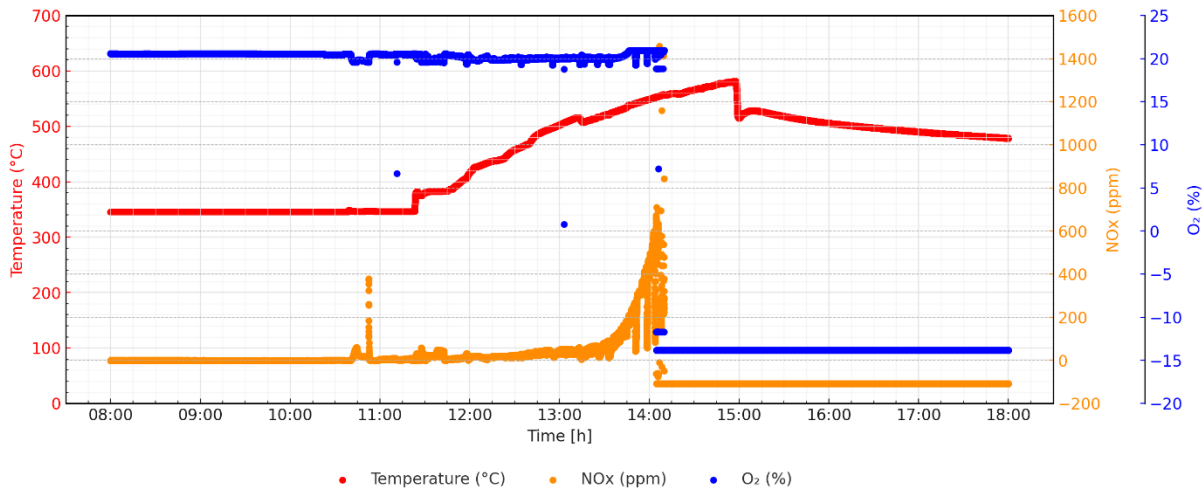


Figure 7: Temperature, NOx Concentration, and O<sub>2</sub> Concentration as a Function of Time on 30.07.2024

According to the operating protocol, the salt pump started at 10:35. At 11:19, flooding of the receiver began, and at 11:25 the system was switched to serpentine flow. From the start of the measurements at 09:00 until about 11:20, the outlet temperature stayed steady around 345–349 °C. In this phase, the NOx signal fluctuated around zero, sometimes slightly positive, sometimes slightly negative, with one spike reaching around 400 ppm before dropping back again. Since there was no gas flow from the facility to the sensor at that time, the spike was most likely caused by the intake of ambient air. Meanwhile, the O<sub>2</sub> readings stayed at normal levels, around 20.6 %.

After 11:20, the outlet tank temperature started to rise steadily and reached its maximum of 580.8 °C at 14:57. During this heating phase, the NOx values stayed irregular without showing any clear link to the temperature rise, while the O<sub>2</sub> signal also remained almost constant. This may be because there was no pressure control during this period and therefore no gas flow passed the sensor.

A striking change happened between 13:30 and 14:06, when NO<sub>x</sub> increased sharply and reached a peak of 1458.8 ppm at 14:06, this rise may be related to the activation of the pressure control system and the first release of gas flow at a higher salt temperature. Just a few minutes later, at 14:09, the NO<sub>x</sub> signal collapsed to about -109 ppm and stayed there for the rest of the day, according to the operating protocol, the pressure control valve stopped switching at that time, which means that no gas flow passed by the sensor anymore. At the same moment, the O<sub>2</sub> signal also failed, after the last normal reading of 20.9 % at 14:09, it suddenly dropped into a negative range of around -13.8 % and did not recover, even as the outlet tank temperature slowly cooled down from 580.8 °C to 478 °C.

The operating protocol also notes drainage took place at 14:58 and, during drainage gas certainly flowed past the sensor, but the sensor signals did not respond and instead remained fixed at their negative values. This clearly indicates that the sensor was not providing plausible measurements values despite the gas flow.

#### **Summary of test day 30.07.2024:**

The analysis of the operating protocol clearly shows that the installed NO<sub>x</sub> sensor did not deliver reliable measurements under CST operating conditions. The NO<sub>x</sub> and O<sub>2</sub> signals were unstable, inconsistent, and in several cases physically impossible. After an initial phase with values fluctuating around zero and a short peak likely caused by ambient air intake, the sensor recorded a sharp rise in NO<sub>x</sub> at 14:06, coinciding with the first gas release at elevated temperature. However, immediately afterwards, both NO<sub>x</sub> and O<sub>2</sub> signals collapsed into negative ranges (down to -109 ppm for NO<sub>x</sub> and -13.8 % for O<sub>2</sub>). Such readings are physically impossible and therefore confirm a malfunction or loss of validity of the sensor response. Even during the drainage event at 14:58, when gas flow past the sensor was certain, the values remained locked in these negative ranges. This demonstrates that the sensor not only failed to track the process conditions but produced erroneous signals, highlighting a fundamental incompatibility of the measurement setup for CST operation.

## Interpretation: 19.08.2024

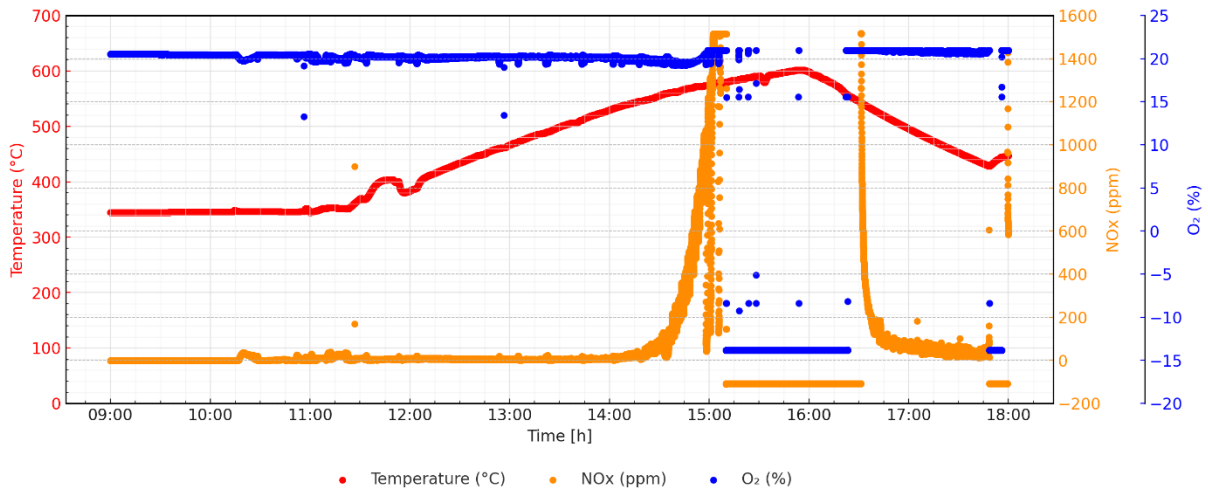


Figure 8: Temperature, NOx Concentration, and O<sub>2</sub> Concentration as a Function of Time on 19.08.2024.

The plant was started at 08:30 and heliostats were focused at 09:10. The salt pump began operation at 09:37, and at 10:52 the receiver was flooded. Between 09:00 and 14:34, the outlet tank warmed from 345 °C to 559 °C, NOx stayed low, and O<sub>2</sub> remained near atmospheric levels. Between 14:34 and 15:09, the outlet tank reached 580 °C. At the same moment, the NOx signal showed a sharp peak of 1514.7 ppm, before dropping again. O<sub>2</sub> values during this period stayed mostly stable in the normal atmospheric range (19.2–20.9%).

After 15:10, the temperature reached 601 °C then decreased to 543 °C, the sensor values collapsed. NOx dropped to a fixed and non-physical baseline around -109 ppm, although a few irregular points still showed spikes up to 1515 ppm. O<sub>2</sub> simultaneously fell into a clearly impossible negative range between -13.8 % and -13.7%.

From 16:31 until the end of the measurement, the outlet tank cooled further to about 428 °C. During this phase, NOx spiked again briefly to around 1516 ppm before immediately falling back into negative values (around -109 ppm). O<sub>2</sub> mostly recovered to normal atmospheric levels between 20.2 % and 21.0 %, but occasional negative readings of about -13.8 % continued to appear.

The operating protocol notes further steps of cooling and shutdown during this late phase. However, the measured signals of NOx and O<sub>2</sub> no longer followed any physical trend. Instead, they show alternating extreme peaks and sustained negative

values, which cannot be explained by the real gas composition.

**Summary of test day 19.08.2024:**

On 19.08.2024, the plant operation and outlet temperature followed the expected course, but the NOx/O<sub>2</sub> sensor gave inconsistent and physically impossible results. The sudden peak of NOx to over 1500 ppm, the simultaneous drop of O<sub>2</sub> into negative ranges, and the fixed negative baselines observed after 15:10 clearly demonstrate a malfunction of the sensor. The measurements from this day cannot be considered reliable.

**Interpretation: 19.09.2024**

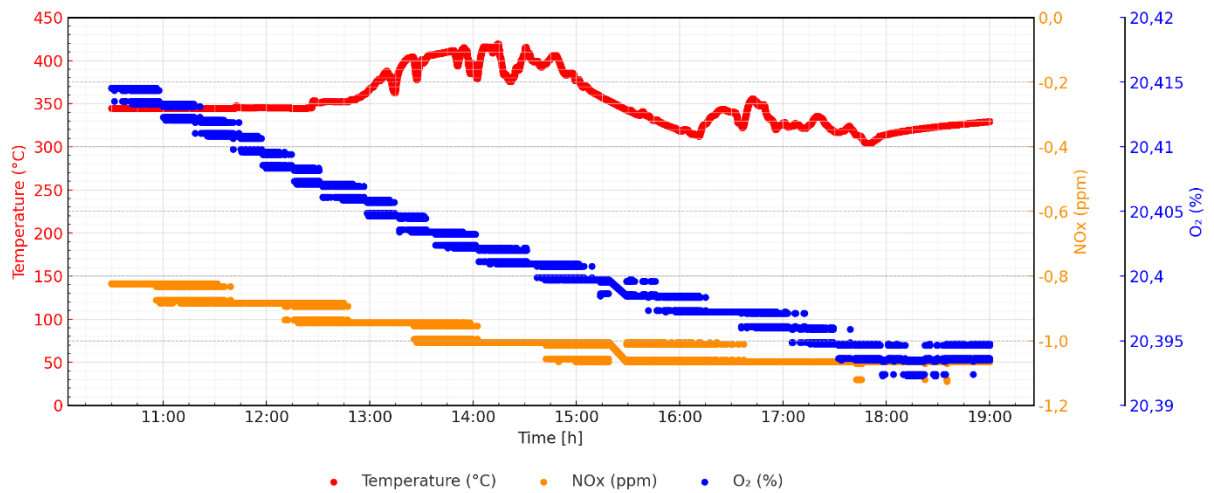


Figure 9: Temperature, NOx Concentration, and O<sub>2</sub> Concentration as a Function of Time on 19.09.2024

For 19.09.2024, the NOx/O<sub>2</sub> sensor did not behave plausibly. NOx values were always negative (−1.126 to −0.823 ppm) and showed no response to heating, load operation, or mass-flow. The system was brought into operation in the morning. The operating protocol notes the salt pump start at 10:49, heliostats focused from 10:53, receiver flooding between 12:22–12:27, switching to load operation at 12:45.

The outlet tank temperature stayed almost flat at around 344 °C. The NOx signal was already negative and close to zero (between −0.82 and −1.12 ppm) and the O<sub>2</sub> reading was very steady (20.4–20.3 %).

After 11:42, the outlet temperature rose gradually and reached its highest value of around 419 °C at 14:14. Despite this heating phase (which includes the period after

flooding and entry into load operation), NO<sub>x</sub> remained entirely negative with no positive values and no peaks (still between  $-1.126$  and  $-0.823$  ppm). O<sub>2</sub> stayed almost stable in the same range ( $\approx 20.39$ – $20.42$  %) and did not show any meaningful reaction to the change in operating conditions.

From 14:14 to the end of the day (19:00) the outlet temperature decreased slowly down to around 304 °C. During this cool-down including the mass-flow steps and further actions listed in the protocol after 17:14, NO<sub>x</sub> continued to read negative only, and O<sub>2</sub> stayed nearly constant around 20.40 %.

### **Summary of test day 19.09.2024:**

The NO<sub>x</sub>/O<sub>2</sub> sensor did not behave plausibly. NO<sub>x</sub> values were always negative ( $-1.126$  to  $-0.823$  ppm) and showed no response to heating, load operation, or mass-flow changes. O<sub>2</sub> remained stable ( $\approx 20.392$ – $20.415$  %). The combination of a fixed negative NO<sub>x</sub> baseline and a nearly unchanging O<sub>2</sub>%, regardless of the operating steps recorded in the protocol, clearly points to a sensor offset/failure.

### **Summary of NO<sub>x</sub> Sensor Behavior:**

Over the course of three test days, the NO<sub>x</sub> sensor consistently showed signs of malfunction and instability when used in the SALSA system.

The sensor occasionally reported negative NO<sub>x</sub> values or displayed sudden, unrealistic jumps and drops, which are physically impossible. These point to problems like calibration, or potential electrical faults.

A noticeable mismatch between NO<sub>x</sub> and O<sub>2</sub> measurements suggests a partial failure limited to the NO<sub>x</sub> sensing pathway possibly affecting the electrode or internal signal processing.

A temperature of around 550°C was achieved only in tests days 30.07.2024 and 19.08.2024, and at this temperature a simultaneous constant negative value in O<sub>2</sub> and NO<sub>x</sub> is measured, suggests that the sensor is no longer functioning above this temperature.

Exposure to gases from salt decomposition appears to affect the sensor's design, raising doubts about its robustness in SALSA conditions.

In short, a sensor developed for automotive exhaust systems doesn't seem well-suited for use in SALSA environments.

## 4. Factors affecting sensor accuracy and alternative measurement concepts

### 4.1 Potential Factor Affecting Sensor Accuracy

The sensing element of the NO<sub>x</sub> sensor used consists of platinum electrodes deposited on a zirconia (ZrO<sub>2</sub>) electrolyte, which enables electrochemical detection of oxygen and nitrogen oxides at high temperature. The stability of platinum electrodes is strongly affected by the presence of alkali cations (Li<sup>+</sup>, Na<sup>+</sup>, K<sup>+</sup>, Cs<sup>+</sup>). It has been shown that the electrochemical dissolution of platinum in alkaline electrolytes follows the sequence Li<sup>+</sup> > Na<sup>+</sup> > K<sup>+</sup> > Cs<sup>+</sup>, indicating that cations with higher atomic number provide greater electrode stability [24].

In molten Solar Salt systems, thermal decomposition produces nitrites and, at advanced stages, alkali oxides (Na<sub>2</sub>O, K<sub>2</sub>O). Although these oxides are non-volatile under CST operating conditions, they can be mechanically entrained in the gas stream as fine aerosols or microdroplets together with O<sub>2</sub> and NO<sub>x</sub> released during salt decomposition. Such salt aerosols may travel through the conduits up to the sensor location [25].

Once deposited, alkali oxide aerosols are considered highly corrosive species. On zirconia-based electrolytes ZrO<sub>2</sub>, they can infiltrate the ceramic surface, impairing ionic conductivity and structural integrity [26]. On platinum electrodes, the combined effect of high temperature and alkali oxides favors the formation of unstable platinum oxides (PtO<sub>2</sub>) and alkali platinates (Na<sub>2</sub>PtO<sub>3</sub>, K<sub>2</sub>PtO<sub>3</sub>), leading to progressive loss of electrocatalytic activity and mechanical stability [27].

Thus, under real CST operating conditions, Solar Salt decomposition may lead to the transport of entrained alkali oxide aerosols, which jointly accelerate the degradation of both ZrO<sub>2</sub> electrolytes and Pt electrodes.

## 4.2 Adapted Techniques for NO<sub>x</sub> Detection under CST Operating Conditions

Choosing the right method for NO<sub>x</sub> measurement in SALSA systems requires careful consideration of the demanding operating environment. High temperatures, reactive gases, and by-products from molten salt decomposition create conditions where robustness and selectivity are critical to ensure reliable data. Under such circumstances, methods like NDIR, chemiluminescence, and NDUV offer the flexibility to detect NO<sub>x</sub> across a broad concentration range from very low levels in ambient monitoring to higher concentrations in process streams.

### Working Principle of NDIR Method

NDIR gas sensors rely on the absorption of infrared radiation by target gas molecules. When IR light passes through the gas, the transmitted intensity decreases according to the Beer–Lambert law (5) [28]:

$$I(\lambda) = I_0(\lambda) \cdot e^{-kx} \quad (5)$$

where  $I_0(\lambda)$  is the initial intensity,  $k$  the absorption coefficient, and  $x$  the product of gas concentration and optical path length.

The sensor evaluates this absorption by comparing detector voltages in reference gas ( $V_0$ ) and target gas ( $V$ ), expressed as the fractional absorbance (6) [28]:

$$FA = (V_0 - V) / V_0 = 1 - e^{-kx} \quad (6)$$

A longer optical path increases sensitivity, making NDIR particularly suitable for detecting gases at low concentrations.

Among the commercially available analyzers based on this measurement principle, two representative models are considered in this work: the Rosemount X-STREAM Enhanced (Figure 10) and the Thermo Scientific Model 60i. Both analyzers require the process gas to be withdrawn from the duct and conditioned through cooling, drying, and filtration before measurement. Their technical specifications, summarized in [Appendix 3](#), include key parameters such as flow rate, inlet pressure limits, conditioning requirements, and detection ranges. These data, provided by the manufacturers, serve as the basis for assessing the potential applicability of the

instruments under the operating conditions of molten salt decomposition in a CST system.

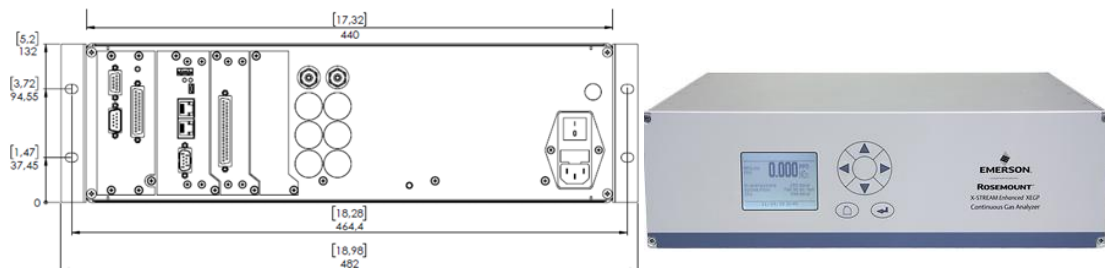


Figure 10: (left drawing and right picture) of the Rosemount X-STREAM Enhanced continuous gas analyzer

### Working Principle of the Chemiluminescence Method

The chemiluminescence method is a widely established technique for the measurement of nitrogen oxides ( $\text{NO}_x$ ) in gas streams. Its operation relies on a specific chemical reaction between nitric oxide ( $\text{NO}$ ) and ozone ( $\text{O}_3$ ). When these two gases interact, nitrogen dioxide ( $\text{NO}_2$ ) is formed in an electronically excited state. As the excited  $\text{NO}_2$  molecules relax back to their ground state, they emit photons in the visible region. The intensity of this emitted light is directly proportional to the concentration of  $\text{NO}$  present in the sample [29].

To quantify the total  $\text{NO}_x$  content ( $\text{NO} + \text{NO}_2$ ), the measurement system typically employs a two-step approach. First,  $\text{NO}$  is measured directly through the chemiluminescence reaction with ozone. Then, in a parallel path, the sample gas is passed through a catalytic converter that reduces  $\text{NO}_2$  to  $\text{NO}$ . The resulting mixture is again subjected to the same chemiluminescence process, providing a signal corresponding to the combined concentration of  $\text{NO}$  and  $\text{NO}_2$ . By calculating the difference between the total  $\text{NO}_x$  signal and the direct  $\text{NO}$  signal, the  $\text{NO}_2$  concentration can be determined with high accuracy [29].

This method provides high sensitivity and selectivity for  $\text{NO}$  and  $\text{NO}_2$  detection, even at trace levels. It is therefore considered one of the most reliable and widely applied techniques for monitoring nitrogen oxides in both environmental and industrial contexts.

In addition to the NDIR analyzers previously discussed two further instruments based on chemiluminescence were reviewed the ECO PHYSICS nCLD 84 M and the KNESTEL TRG CLD (Figure 11). Since these instruments operate in extractive mode, the exhaust gas must be withdrawn from the gas pipe and directed through a sampling line to the analyzer. A detailed comparison of the ECO PHYSICS nCLD 84 M and the KNESTEL CLD analyzers is provided in [Appendix 4](#). The table summarizes key operational parameters such as sample flow requirements, inlet pressure ranges, gas conditioning needs, and detection limits. Referring to this overview facilitates the assessment of sensor compatibility under the specific conditions of molten salt decomposition in the SALSA environment. The operational details presented here are based on the technical datasheets provided by the manufacturers

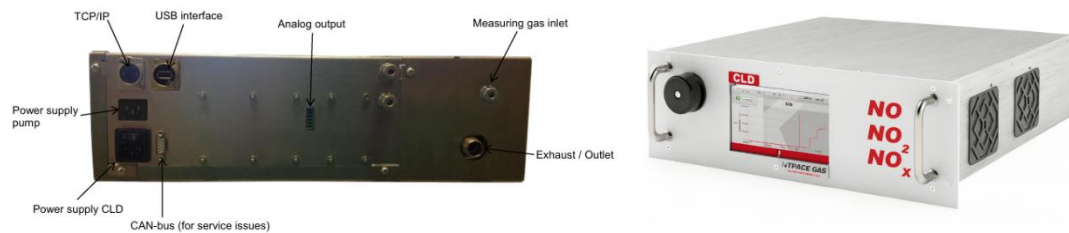


Figure 11: The external design of KNESTEL CLD, illustrating the front and rear view of the instrument.

The internal gas flow of the instrument is depicted in Figure 12. The schematic illustrates the sequence of components through which the sample gas is processed, including filtration, conversion, and the reaction chamber where the chemiluminescence process occurs. This layout ensures a stable and reproducible measurement of NO and NO<sub>2</sub>

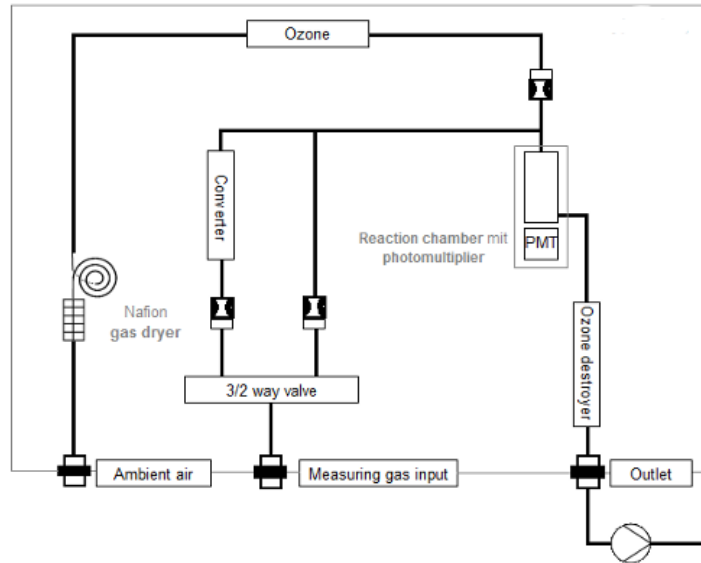


Figure 12: Schematic of the gas flow in KNESTEL CLD analyzer

### Working Principle of NDUV Method

The non-dispersive ultraviolet (NDUV) method measures gas concentrations by exploiting the fact that molecules selectively absorb UV light at characteristic wavelengths. A gas sample is introduced into a measuring cell and irradiated with UV radiation. The intensity of the transmitted light is compared to that of a reference channel containing a clean gas, which allows accurate correction for baseline shifts, lamp fluctuations, and potential interferences. Because NO and NO<sub>2</sub> exhibit distinct absorption bands in the UV range, their concentrations can be quantified using the Beer–Lambert law (5). Advanced NDUV analyzers often apply multi-wavelength analysis and spectral separation to improve selectivity and minimize the impact of temperature, humidity, or interfering absorption from other gases. Thanks to its high precision, rapid response, and relatively low maintenance, NDUV is widely applied for real-time monitoring of NO<sub>x</sub> in industrial emissions, ambient air, and laboratory settings [28].

Beyond the NDIR and CLD instruments already discussed, this work also examines two analyzers that use ultraviolet (UV) absorption as their measurement principle: the SICK GM32 and the Siemens SIPROCESS UV600 (Figure 13). While both rely on UV-based detection, they differ significantly in design. The GM32 is an in-situ device, performing measurements directly inside the gas duct, whereas the UV600

is an extractive analyzer that requires the gas to be withdrawn, cooled, and conditioned before analysis. Their key specifications are summarized in [Appendix 5](#), using data drawn from the manufacturer's technical documentation.



Figure 13: Left: UV-based gas analyzers (SICK GM32) directly in-situ installed. Right: Front view of Siemens SIPROCESS UV600.

### Working principle of electrochemical Method

As previously explained, the electrochemical measurement principle of the NO<sub>x</sub> sensor (70501) remains the same. Below, we compare two additional sensors based strictly on the specifications provided by the manufacturers. The HTK GSE 400 operates on a diffusion principle and can only be placed at the outlet of the exhaust duct; it is waterproof, which allows outdoor installation, but it is not suitable for in-situ process measurements. By contrast, the MSA PrimaX is designed for in-situ monitoring. Their detailed characteristics are summarized in [Appendix 6](#).



Figure 14. NO<sub>x</sub> sensors: MSA PrimaX (left) and HTK GSE 400 (right)

To provide a clear comparison, the main characteristics of the three methods are summarized in the following tables (2,3).

<b>Method</b>	<b>Description</b>
<b>NDIR (Non-Dispersive Infrared)</b>	Uses infrared light absorption to detect gases. The method tracks how much IR radiation is absorbed at specific wavelengths, a principle widely applied for gases such as CO <sub>2</sub> and also used for NO <sub>x</sub> .
<b>Chemiluminescence</b>	Determines gas concentration by measuring the light produced during a chemical reaction. The brightness of the emitted light is directly linked to the amount of gas present.
<b>NDUV (Non-Dispersive Ultraviolet)</b>	Measures gases by their ability to absorb ultraviolet light at defined wavelengths. Highly selective for gases like NO <sub>2</sub> , but readings can be influenced by other compounds that also absorb UV.

Table 2: Overview of Selected NO<sub>x</sub> Measurement Methods

Criteria	Chimiluminescence	NDIR (Non-Dispersive Infrared)	NDUV (Non-Dispersive Ultraviolet)
<b>Sensitivity</b>	Extremely high, able to detect at ppb levels.	Good for ppm-range detection, reliable for continuous use but less effective at very low concentrations.	High sensitivity from ppb to ppm with fast response time.
<b>Cost</b>	Purchase and maintenance costs are high.	Purchase is very high, and low running costs.	Less costly than Chemiluminescence, but still pricier than electrochemical sensors.
<b>Selectivity</b>	Very selective for NO and NOx.	Works well for common gases, but cross-sensitivity with other IR-absorbing species can occur.	Strong ability to distinguish NO and NO <sub>2</sub> ; some risk of interference from other UV absorbers.
<b>Stability</b>	Stable under laboratory conditions, but field use requires filters and ozone systems.	Good resistance to temperature variations, though detectors can drift over time.	Reliable over a wide range of temperatures, but requires stable light sources and periodic optics care.
<b>Precision</b>	Delivers reference-grade accuracy.	High precision for medium and high concentrations; less accurate at very low levels.	Very precise, especially for continuous monitoring.
<b>Measurement</b>	Automatic measurements, though drying and filtration are required	Provides fast, direct readings.	Allows, continuous, monitoring, but requires occasional cleaning of optical components.

Table 3: Comparative Overview of NO<sub>x</sub> Measurement Methods [28]

### 4.3 Proposed Measurement Concept:

After reviewing different NO<sub>x</sub> analyzers based on the main measurement methods available on the market, a concept has been found that is better suited to the specific conditions of SALSA. The selection was guided by criteria such as measurement accuracy, detection limits, robustness under demanding conditions, and the need to protect the equipment from potential damage.

In a SALSA, gases originating from the thermal decomposition of nitrates flow at high temperatures and may contain solid contaminants or reaction products that can interfere with measurement or reduce sensor lifetime. These harsh conditions also pose a risk of fouling and deposits on sensitive surfaces, which can compromise reliability.

The proposed concept is designed to ensure representative and stable measurements while minimizing these risks. To achieve this, it incorporates gas conditioning including cooling, filtration, and controlled sampling before the gas reaches the analyzer. In this way, both the accuracy and durability of the measurement system can be maintained, even in the challenging environment of molten-salt loops.

The simplified diagram below (Figure 15) illustrates the principle, while the detailed technical aspects, such as gas conditioning steps and calibration procedures, are presented in the following sections.

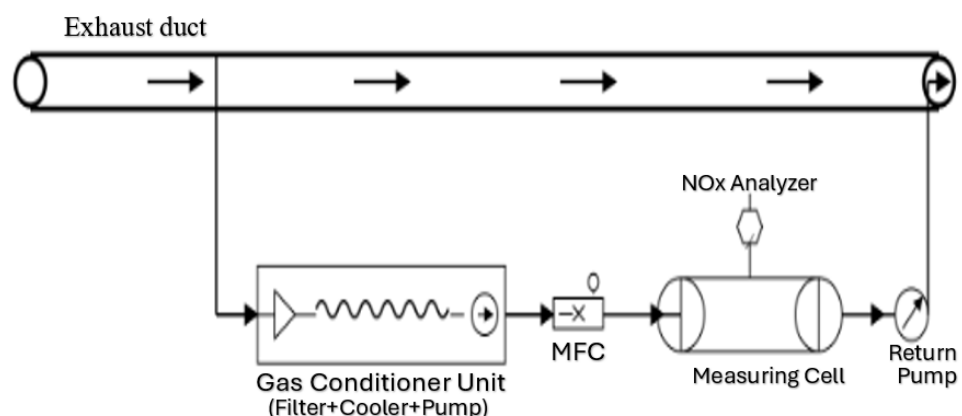


Figure 15: NO<sub>x</sub> Measurement Concept with Gas Conditioning Unit and Closed-Loop Operation

The Gas Conditioning Unit, which combines a filter, cooler, and pump, plays a central role in this process. The pump extracts the sample from the duct, while the filter removes solid particles and the cooler reduces the gas temperature to within the admissible range of the sensor and condenses excess humidity. This ensures that the sample is clean, dry, and stable, thereby protecting the measuring cell from contamination and premature degradation.

The conditioned gas then passes through a Mass Flow Controller (MFC). The MFC regulates the flow precisely and compensates for upstream or downstream pressure fluctuations. This stabilization is critical to guarantee reproducible measurements and to comply with the manufacturer's requirements for the analyzer's inlet conditions.

Subsequently, the gas enters the measuring cell, where the NO<sub>x</sub> analyzer determines the concentration of nitrogen oxides (depending on the selected technology, e.g., electrochemical, NDIR, UV, or CLD). After the measurement, a return pump directs the gas back into the exhaust duct. In this way, the system operates in a closed-loop configuration: no emissions are released into the environment, and the overall mass balance of the process remains unchanged.

This concept addresses the key challenges of CST environments high gas temperatures, solid contaminants, and chemically reactive species by ensuring that the analyzer receives a controlled and representative gas stream. It thus combines measurement reliability with instrument protection, which is essential for long-term operation in molten-salt applications.

## **5. Conclusion:**

The objective of this thesis was to evaluate the reliability of the currently installed NO<sub>x</sub> sensor in the SALSA molten salt loop and to identify potential sources of error, while also exploring alternative methods suitable for continuous NO<sub>x</sub> detection under Concentrated Solar Tower (CST) operating conditions.

The theoretical part provided the necessary framework by describing the role of the binary nitrate mixture NaNO<sub>3</sub>/KNO<sub>3</sub> as heat transfer and storage medium, its thermal stability limits, and the associated decomposition pathways leading to the formation of reactive gases, including NO and NO<sub>2</sub>. Furthermore, the risks

associated with the presence of  $\text{NO}_x$  in terms of safety, corrosion, and environmental impact were discussed in relation to the operational context of the SALSA facility.

In the experimental section, the focus was placed on the electrochemical  $\text{NO}_x$  sensor currently in use. The analysis of several measurement campaigns revealed recurring anomalies, including consistently negative readings. These findings clearly indicate that the current sensor is not suitable for accurate detection of  $\text{NO}_x$  in molten salt environments. Additional considerations were given to factors potentially affecting sensor accuracy, such as electrode degradation.

Based on these results, alternative technologies were evaluated, including NDIR, chemiluminescence, and NDUV analyzers. Each method was assessed in terms of working principle, strengths, limitations, and feasibility under CST conditions. This comparative analysis demonstrated that while no single method is free of challenges, more robust solutions exist compared to the current setup, provided that appropriate gas conditioning (cooling, filtration, flow regulation) is ensured.

Building on these insights, a measurement concept was proposed that integrates with an adapted gas conditioning unit. The concept aims to guarantee reliable and continuous monitoring of  $\text{NO}_x$  emissions in the SALSA loop, thereby enabling both safer operation of the facility and improved understanding of the chemical processes involved in nitrate decomposition.

In conclusion, this thesis demonstrated that the sensor currently in place is fundamentally unsuited for CST applications and should be replaced by a more reliable technology. The proposed concept represents a significant step toward establishing a robust  $\text{NO}_x$  monitoring strategy in molten salt environments. Future work will consist in installing and operating such an analyzer at the SALSA facility, validating its performance under real conditions.

## 6. Reference

- [1] Ferruzzi G, Delcea C, Barberi A, Di Dio V, Di Somma M, Catrini P, Guarino S, Rossi F, Parisi ML, Sinicropi A, et al. Concentrating Solar Power: The State of the Art, Research Gaps and Future Perspectives. *Energies*. 2023;16(24):8082. doi:10.3390/en16248082.  
<https://www.mdpi.com/1996-1073/16/24/8082>.
- [2] Frantz C, Binder M, Sibum M, Reisch I, Schuhbauer C. Basic engineering of a high-performance molten salt tower receiver system. *Basic Engineering of a High Performance Molten Salt Tower Receiver System*
- [3] Wei, X., Yang, C., Lu, J., Wang, W., & Ding, J., 2017, "The mechanism of NO<sub>x</sub> emissions from binary molten nitrate salts in thermal energy storage processes," *Applied Energy*, 207, pp. 265–273. <https://doi.org/10.1016/j.apenergy.2017.06.109>
- [4] DLR Jülich, Internal document: Commissioning of a solar Test Setup for Central Receiver Operation at 600 °C
- [5] Pflieger N, et al. Sensibel energy storage in anhydrous molten salts/nitrates. *Beilstein Journal of Nanotechnology*. 2015;6:154–172. doi:10.3762/bjnano.6.154.  
<https://www.beilstein-journals.org/bjnano/articles/6/154>
- [6] Bonk A, Bauer T. Solar Salt Thermal Property Analysis Report. Deutsches Zentrum für Luft- und Raumfahrt (DLR). 2021.  
[https://elib.dlr.de/143749/1/PropertyAnalysis\\_SQM-DLR\\_final%20Report\\_v2.1.pdf](https://elib.dlr.de/143749/1/PropertyAnalysis_SQM-DLR_final%20Report_v2.1.pdf)
- [7] Liu Z. Heat Transfer Materials for Next Generation Concentrated Solar Power Systems. Technical Report. 2025. [https://www.researchgate.net/figure/Density-curves-of-solar-salt-and-TMS-2\\_fig3\\_380623057](https://www.researchgate.net/figure/Density-curves-of-solar-salt-and-TMS-2_fig3_380623057)
- [8] Caraballo A, Lainez R, Cabeza LF. Molten Salts for Sensible Thermal Energy Storage. *Energies*. 2021;14(4):1197. doi:10.3390/en14041197  
<https://www.mdpi.com/1996-1073/14/4/1197>
- [9] Guerreiro L, Henríquez M. High Temperature Sensible Storage – Molten Salts. In: *Encyclopedia of Energy Storage*. Elsevier; 2022.  
[https://dspace.uevora.pt/rdpc/bitstream/10174/35212/1/Book%20Chapter\\_High%20Temperature%20-%20Molten%20Salts%20-%20GuerreiroL%20HenriquezM.pdf](https://dspace.uevora.pt/rdpc/bitstream/10174/35212/1/Book%20Chapter_High%20Temperature%20-%20Molten%20Salts%20-%20GuerreiroL%20HenriquezM.pdf)
- [10] Prieto C, Lopez-Roman A, Cabeza LF. Experimental evaluation of the thermal degradation of Solar Salt under different gas covers. *Journal of Energy Storage*. 2023; 72: 108412. doi: 10.1016/j.est.2023.108412.  
<https://www.sciencedirect.com/science/article/pii/S2352152X23018091>
- [11] Nissen, D. A., 1981. The Chemistry of the Binary NaNO<sub>3</sub>–KNO<sub>3</sub> System. U.S. Department of Energy, OSTI Report. Available at:  
<https://www.osti.gov/servlets/purl/6349401>
- [12] Wright S, Tran T, Chen C, Olivares R, Sun S. Thermal stability of potassium and sodium nitrate molten salt mixtures above 500 °C. CSIRO (2012).  
<https://www.pyrometallurgy.co.za/MoltenSlags2012/W074.pdf>
- [13] Screening tests of sodium nitrate and potassium nitrate" by C. M. Kramer, published in *Materials and Energy Research*, 1982  
<https://www.sciencedirect.com/sdfe/pdf/download/eid/1-s2.0-0038092X82900822/first-page-pdf>
- [14] Prieto C, Ruiz-Cabañas FJ, Rodríguez-Sánchez A, Rubio-Abujas C, Fernández-Inés AI, Martínez M, et al. Effect of the impurity magnesium nitrate in the thermal decomposition of the solar salt. *Solar Energy*. 2019;192:186–192.

doi:10.1016/j.solener.2018.08.046.

<https://www.sciencedirect.com/science/article/abs/pii/S0038092X18308168>

[15] HeliosCSP. Oxygen Fix for High-Temperature Molten Salt Degradation and Corrosion at 620 °C. HeliosCSP News. 2022.

<https://helioscsp.com/oxygen-fix-for-high-temperature-molten-salt-degradation-and-corrosion-at-620c/>

[16] Bonk A, Kumar S, Braun M, Hanke A, Klein S, Müller J, Bauer T. Thermal Energy Storage using Solar Salt at 620 °C: How a reactive gas atmosphere mitigates corrosion of structural materials

<https://www.solarpaces.org/wp-content/uploads/Thermal-Energy-Storage-using-Solar-Salt-at-620-%C2%B0C-How-a-reactive-gas-atmosphere-mitigates-corrosion-of-structural-materials.pdf>

[17] Jung, C., & Spenke, C., 2024. Volumetric Determination of Densities of Molten Salts for CSP Applications. SolarPACES Conference Proceedings 2023, v.2.

<https://doi.org/10.52825/solarpaces.v2i.914>

[18] Health and Environment Alliance (HEAL), 2023. The health impacts of nitrogen dioxide (NO<sub>2</sub>) pollution. Available at: [https://www.env-health.org/wp-content/uploads/2023/06/NO2\\_briefing\\_EN.pdf](https://www.env-health.org/wp-content/uploads/2023/06/NO2_briefing_EN.pdf)

[19] Agency for Toxic Substances and Disease Registry (ATSDR), 2002. Nitrogen Oxides (Nitric Oxide, Nitrogen Dioxide, Etc.) – ToxFAQs. Available at:

<https://www.atsdr.cdc.gov/toxfaqs/tfacts175.pdf>

[20] European Environment Agency (EEA), 2024. Air pollution in Europe: 2024 reporting status under the National Emission Reduction Commitments Directive.

Available at: <https://www.eea.europa.eu/en/analysis/publications/national-emission-reduction-commitments-directive-2024>

[21] Federal Ministry for the Environment, Nature Conservation, Nuclear Safety and Consumer Protection (BMUV), First General Administrative Regulation Pertaining the Federal Immission Control Act (Technical Instructions on Air Quality Control – TA Luft). Berlin: BMUV, 2021.

[https://www.bmuv.de/fileadmin/Daten\\_BMU/Download\\_PDF/Luft/taluft\\_engl.pdf](https://www.bmuv.de/fileadmin/Daten_BMU/Download_PDF/Luft/taluft_engl.pdf)

[22] EngineSens Motorsensor GmbH, Internal document: Manual / technical specification NO<sub>x</sub> Sensor 1500ppm, Part.-No. 70501

[23] MAN Energy Solutions DWE® Reactors – Deggendorf, Internal document: Auslass-Leitung hinter den Save-Loc Behältern RPM30 BR001 ; RPM50 BR007

[24] Cation Effect on the Electrochemical Platinum Dissolution. Journal of the American Chemical Society, 2025, 147 (5), 4667-4674. DOI: 10.1021/jacs.4c17833.

[https://pubs.acs.org/doi/pdf/10.1021/jacs.4c17833?ref=article\\_openPDF](https://pubs.acs.org/doi/pdf/10.1021/jacs.4c17833?ref=article_openPDF)

[25] Shahbazi, K.; Kraus, A.; Gerstl, S.; Pfrang, A.; Krauss, F. State of Knowledge on Aerosols and Bubble Transport for Molten Salt Reactors. Argonne National Laboratory Report, ANL/CFCT-22/34, 2022.

<https://publications.anl.gov/anlpubs/2022/10/178853>

[26] Espinoza-Medina, R.; De La Torre, D.; Zeng, J.; Fuentes, A. F.; Kinnart, F.; Benes, N. E. Corrosion Behavior of ZrO<sub>2</sub> and YSZ in Molten FLiNaK Salt. MRS Advances 2022, 7(32–33), 1731–1738. DOI: 10.1557/s43580-022-00241-3.

[https://www.researchgate.net/publication/358443725\\_Corrosion\\_behavior\\_of\\_ZrO2\\_and\\_YSZ\\_in\\_molten\\_FLiNaK\\_salt](https://www.researchgate.net/publication/358443725_Corrosion_behavior_of_ZrO2_and_YSZ_in_molten_FLiNaK_salt)

- [27] Kasuya, M.; Iwase, A.; Shimada, M. Alkali Metal Platinates Synthesized by the Calcination of Pt Black and Alkali Metal Carbonates. *Journal of the Ceramic Society of Japan* 2013, 121(1418), 983–989. DOI: 10.2109/jcersj2.121.983. [https://www.jstage.jst.go.jp/article/jcersj2/121/1418/121\\_JCSJ-P13115/\\_pdf](https://www.jstage.jst.go.jp/article/jcersj2/121/1418/121_JCSJ-P13115/_pdf)
- [28] Zhao, Y.; Zhang, C.; Ci, G.; Zhao, X.; Lv, J.; Liang, J.; Ming, A.; Wei, F.; Mao, C. Development of High-Precision NO<sub>2</sub> Gas Sensor Based on Non-Dispersive Infrared Technology. *Sensors* 2024, 24(13), 4146. DOI: 10.3390/s24134146. <https://www.mdpi.com/1424-8220/24/13/4146>
- [29] Banasiewicz, A.; Janicka, A. *Selection of a Universal Method for Measuring Nitrogen Oxides in Underground Mines: A Literature Review and SWOT Analysis*. *Atmosphere* 2025, 16(9), 1051. DOI: 10.3390/atmos16091051. <https://www.mdpi.com/2073-4433/16/9/1051>.

## 7. Appendix

### Appendix 1

Function	Description
Signal conditioning	Amplifies, filters, and stabilizes raw signals from electrodes.
Control of pumping currents	Controls oxygen and NOx pumping cells (Ip0, Ip1, Ip2).
Voltage regulation	Maintains correct voltages across sensor cells (V0, V1, V2, Vref).
Heater control assistance	Supports heater current control (usually supervised by ECU).
Temperature compensation	Corrects signals based on internal sensor temperature.
Cross sensitivity compensation	Adjusts for gas interferences (O <sub>2</sub> , H <sub>2</sub> , NH <sub>3</sub> , etc.).
Analog to digital conversion (ADC)	Converts analog currents and voltages into digital signals.
Communication with ECU	Packages the measurement into CAN messages for the ECU.

Table 4: Overview of control signals and their functions in the electrochemical NOx sensor.

### Appendix 2

Function	Description
Power Supply	Provides voltage and current to the sensor and ASIC.
Heater Control	Regulates sensor element temperature based on feedback.
Communication	Sends sensor data to “vehicle systems “via CAN bus.
Diagnostics	Monitors sensor status, errors, and health.
Data Validation	Checks ASIC data for plausibility and consistency.
Safety Management	Disables sensor in case of critical failures.

Table 5: Main functions of the Electronic Control Unit (ECU) for NOx sensor operation.

### Appendix 3

<b>Criteria</b>	<b>Rosemount X-STREAM Enhanced</b>	<b>Thermo Scientific Model 60i</b>
<b>Sampling mode</b>	Extractive (gas is taken out of the duct and measured in the analyzer)	Extractive (gas is taken out of the duct and measured in the analyzer)
<b>Integrated pump</b>	Optional, depending on configuration	Yes – built-in pump
<b>External pump required</b>	Yes, if no internal pump option is installed	No
<b>Sample flow rate</b>	0.2–1.5 L/min	≥ 1.0 L/min
<b>Inlet pressure range</b>	Up to 1500 mbar absolute (7 psig)	At atmospheric pressure
<b>Max. gas temperature / remarks</b>	Needs cooling and drying before analysis; sample dew point must be at least 10 K below analyzer temperature	Needs cooling and drying before analysis; dew point must be 2–8 °C
<b>Filtration / gas conditioning</b>	External particle filter (2 µm) and water-droplet filter (coalescence filter) required	External cooler and particle filters (≤ 1 µm) required to remove dust and moisture



<b>Detection limit (LOD)</b>	NO: as low as 100 ppm; NO <sub>2</sub> : as low as 25 ppm	NO: ~0.5 ppm
<b>NO<sub>x</sub> measuring range</b>	NO: 0–100 ppm up to 0–100 %; NO <sub>2</sub> : 0–25 ppm up to 0–10 %; NO <sub>x</sub> calculated as NO + NO <sub>2</sub>	NO up to ~1000 ppm; NO <sub>x</sub> calculated from NO and NO <sub>2</sub>
<b>Response time</b>	4–7 s (t <sub>90</sub> )	~70 s (t <sub>90</sub> )
<b>Maintenance / calibration</b>	Automatic zero and span checks possible with external valves	Built-in valves for zero/span checks; works with Thermo 61i calibrator for NO <sub>2</sub>

Table 6: Technical comparison of infrared analyzers (Rosemount X-STREAM Enhanced vs. Thermo Scientific Model 60i).

#### Appendix 4

<b>Criteria</b>	<b>ECO PHYSICS nCLD 84 M</b>	<b>KNESTEL CLD</b>
<b>Sampling mode</b>	Extractive, gas sample transported to reaction chamber	Extractive, gas sample transported to reaction chamber
<b>Integrated pump</b>	Yes (internal membrane pump included)	No (in the offered version)
<b>External pump required</b>	No	Yes, external membrane pump recommended (KNF 920 Vacuum)
<b>Sample flow rate</b>	≈ 1.0 L·min <sup>-1</sup>	≈ 0.5 L·min <sup>-1</sup>

<b>Inlet pressure range</b>	600–1200 mbar; optional electro-mechanical pressure regulation module available	800–1100 mbar; pressure controlled by internal by-pass valve
<b>Max. gas temperature / remarks</b>	Can handle “hot and humid” gases without external cooler, but condensation must be avoided	Gas temperature limited to 15–35 °C; external drying required (dew point $\leq 5$ °C)
<b>Filtration / gas conditioning</b>	Integrated sample gas filter; internal drying unit included	No sufficient internal filter; fine external filtration $<0.1$ $\mu\text{m}$ required; optional built-in dryer available
<b>Detection limit</b>	0.012 ppm	0.05 ppm
<b>NO<sub>x</sub> measuring range</b>	Configurable ~5–500 ppm	Up to ~250 ppm (up to 10,000 ppm with external O <sub>2</sub> source)
<b>Response time</b>	Very fast ( $T_{90} < 1$ s)	2–30 s depending on filter settings
<b>Maintenance / NO<sub>2</sub> converter</b>	Integrated converter, automatic calibration possible	Converter replaceable from the front, easy maintenance
<b>Ozone source</b>	Internally generated from dry air (no external gas supply required)	Internally generated from ambient air; external O <sub>2</sub> cylinder required for high concentration ranges

Table 7: Technical comparison of chemiluminescence analyzers (ECO PHYSICS nCLD 84 M vs. KNESTEL TRG CLD MB 1).

<b>Criterion</b>	<b>Sick GM32</b>	<b>Siemens SIPROCESS UV600</b>
<b>Sampling mode</b>	In-situ (direct measurement in gas duct, DOAS UV)	Extractive (sample withdrawn and conditioned, NDUV)
<b>Sample flow rate</b>	Not applicable (no extraction, direct in-duct measurement)	20–120 L/h ( $\approx$ 0.33–2.0 L/min)
<b>Inlet pressure range</b>	Not applicable (in-situ)	–200 ... +300 hPa relative
<b>Max. gas temperature</b>	Up to 550 °C (standard), 650 °C (option)	5–55 °C (after cooling/conditioning)
<b>Gas conditioning / filtration</b>	Not required (direct optical path, self-alignment)	Requires external cooling, drying, and particle filtration
<b>Integrated pump</b>	No (not needed for in-situ)	Optional internal membrane pump (C15)
<b>External pump required</b>	No	Yes, if no internal pump option is installed
<b>NO<sub>x</sub> measuring range</b>	NO: 0–40 up to 0–1,900 ppmv; NO <sub>2</sub> : 0–50 up to 0–1,000 ppmv	NO: 0–10 up to 0–1,000 ppmv; NO <sub>2</sub> : 0–10 up to 0–1,000 ppmv. NO <sub>x</sub> calculated as NO + NO <sub>2</sub>

<b>Detection limit (LOD)</b>	Application-dependent; ranges certified for CEMS (QAL1)	Smallest span: 0–10 ppmv (requires stable, thermostated conditions)
<b>Response time (t<sub>90</sub>)</b>	≥ 5 s (open probe, cross-duct); ≥ 120 s (gas-testable probe); adjustable	Not specified in datasheet (no explicit t <sub>90</sub> value given)
<b>Maintenance / calibration</b>	Automatic optical alignment, QAL3 self-checks, long maintenance intervals	UV lamp lifetime ≈ 2 years; zero/span calibration with gases; replaceable filters and lamp

Table 8: Technical comparison of Sick GM32 vs Siemens SIPROCESS UV600

Appendix 6:

<b>Criterion</b>	<b>MSA PrimaX (P / I)</b>	<b>HTK GSE 400</b>
<b>Sampling mode</b>	Diffusion in-situ (gas diffuses through membrane)	Diffusion
<b>Inlet pressure range</b>	Ambient (80–110 kPa)	Ambient (not specified, diffusion principle)
<b>Max. gas temperature / remarks</b>	Sensor NO: –15...40 °C; NO <sub>2</sub> : –20...50 °C; Device –40...70 °C	Device: –20...50 °C
<b>Filtration / gas conditioning</b>	Accessories available (pump adapter, duct adapter)	Ambient diffusion only, not suitable for direct in-duct sampling

<b>Detection limit (LOD)</b>	Resolution: NO 1 ppm, NO <sub>2</sub> 0.1 ppm (0–10 ppm range)	Not specified (only “high accuracy, low cross-sensitivity”)
<b>NO<sub>x</sub> measuring range</b>	NO: 0–100 ppm; NO <sub>2</sub> : 0–10 / 0–20 / 0–100 ppm (separate measurement, no direct NO <sub>x</sub> sum)	Specific ranges available on request
<b>Maintenance / calibration</b>	Regular calibration gas recommended;	Maintenance every 6 months max; recalibration required after >4 weeks downtime

Table 9: Technical comparison of MSA PrimaX (P / I) vs HTK GSE 400